University of Groningen

Flexible constraints

Hess, Berk; Saint-Martin, Humberto; Berendsen, Herman J. C.

IMPORTANT NOTE: You are advised to consult the publisher's version (publisher's PDF) if you wish to cite from it. Please check the document version below.

Document Version
Publisher's PDF, also known as Version of record

[Link to publication in University of Groningen/UMCG research database](#)

Flexible constraints: An adiabatic treatment of quantum degrees of freedom, with application to the flexible and polarizable mobile charge densities in harmonic oscillators model for water

Berk Hess, Humberto Saint-Martin, and Herman J. C. Berendsen

Flexible constraints: An adiabatic treatment of quantum degrees of freedom, with application to the flexible and polarizable mobile charge densities in harmonic oscillators model for water

Berk Hess[a)]
Department of Biophysical Chemistry, Rijksuniversiteit Groningen, Nijenborgh 4, 9747 AG Groningen, The Netherlands

Humberto Saint-Martin
Centro de Ciencias Físicas, Universidad Nacional Autónoma de México, Apartado Postal 48-3, 62251 Cuernavaca, Morelos, México

Herman J. C. Berendsen
Department of Biophysical Chemistry, Rijksuniversiteit Groningen, Nijenborgh 4, 9747 AG Groningen, The Netherlands

In classical molecular simulations chemical bonds and bond angles have been modeled either as rigid constraints, or as nearly harmonic oscillators. However, neither model is a good description of a chemical bond, which is a quantum oscillator that in most cases occupies the ground state only. A quantum oscillator in the ground state can be represented more faithfully by a flexible constraint. This means that the constraint length adapts itself, in time, to the environment, such that the rotational and potential forces on the constraint cancel out. An accurate algorithm for flexible constraints is presented in this work and applied to study liquid water with the flexible and the polarizable "mobile charge densities in harmonic oscillators" model. The iterations for the flexible constraints are done simultaneously with those for the electronic polarization, resulting in negligible additional computational costs. A comparison with fully flexible and rigidly constrained simulations shows little effect on structure and energetics of the liquid, while the dynamics is somewhat faster with flexible constraints. © *2002 American Institute of Physics.* [DOI: 10.1063/1.1478056]

I. INTRODUCTION

The theoretical description of large molecular systems with atomic detail is now routinely done by means of numerical simulations, using molecular dynamics (MD) with classical equations of motion, or the Monte Carlo (MC) method with classical statistical thermodynamics.[1,2] Within this context, chemical bonds and bond angles have been properly treated[3] as rigidly constrained to some equilibrium value,[4–6] and the possible effects of flexibility, as well as those of polarizability, have been included in an average way (or "parametrized away")[7] by fitting the analytical interaction potentials to reproduce bulk properties. This has allowed for very simple expressions that are cheap to evaluate, and have shown their ability to perform rather well, in some cases even for thermodynamic states quite different from those used in the fitting of the parameters. However, there are cases where the flexibility of even small molecules, as water, is likely to be relevant,[8,9] such as the hydration of ions,[10,11] especially under narrow confinement as in the filters of ion channels.[12,13] Therefore, there is a number of water models that include specific terms for the stretching and compressing of bond lengths and angles, with varying degrees of complexity.[9,14–19]

The explicit inclusion of flexibility brings about several problems:[3] (1) Because intramolecular vibrations are much faster than translations and rotations, numerical simulations have to be refined with shorter time steps in molecular dynamics, and with a more frequent sampling of deformations in Monte Carlo; (2) the presence of weakly coupled modes of different frequencies makes the redistribution of energy among them a very slow process, thus requiring a long equilibration period; and (3) the quantum nature of fast intramolecular vibrations cannot be neglected because their frequencies ν are in a range where $h\nu \gg k_B T$ for a wide range of temperatures T, h being Planck's constant and k_B Boltzmann's constant. One way to deal with these problems in MD is to use a multistep approach, where the quantum degrees of freedom are treated with a path-integral formulation (PIMD),[20,21] following classical trajectories of quasiparticles involved in those degrees of freedom.[22–25] This approach has already been applied in studies of liquid water;[26–30] however, it is computationally expensive, thus preventing the possibility of longer simulations for larger systems that would be needed to compute properties that are slow to converge. Therefore, an alternative method is needed, which overcomes the problems of short time steps and long equilibration period, and allows quantum corrections to be applied afterwards.

In this paper we show that quantum degrees of freedom can be replaced by flexible constraints (i.e., these degrees

---

[a)]Author to whom correspondence should be addressed; electronic mail: hess@chem.rug.nl

of freedom are constrained at values where the net generalized forces acting on them vanish) under the conditions that the quantum oscillators remain in their ground state and have constant zero-point energies. A formulation to treat self-consistent flexible constraints has recently been proposed by Zhou et al.[31] However, the two methods derived from it are limited to harmonic bond potentials and consider only linear intermolecular effects on the bonds and bond angles, thus providing approximate solutions to the equations of motion.[32] In this paper we present a similar, but more general method, that works for any combination of coupled constraints and includes the total force acting in the direction of the bond, with the additional asset that the evaluation of rotational forces does not require complicated mathematics, because they are calculated from constraint displacements. The theoretical background and the derivation of the method are presented in Sec. II. In Sec. III, we show the algorithm as implemented in the GROMACS[33] package. In Sec. IV, we present the performance of the method for a simple two-dimensional test system, and in Sec. V, we apply the method to MD simulations of liquid water with the ''mobile charge densities in harmonic oscillators'' (MCDHO) model,[34] and compare the results to a recent path-integral MD made with the same model.[30] It should be stressed, though, that the aim of this work is not to refine the MCDHO model, but to use it for the application of the flexible constraints method.

II. THE METHOD

Because chemical bonds have vibrational frequencies well above $k_B T/\hbar$, they are best described by quantum oscillators in their respective ground states. In this section we show that a faithful, i.e., thermodynamically correct, classical description can be obtained by replacing such quantum degrees of freedom by flexible constraints.

We consider a conservative system of N interacting particles described by generalized coordinates $q_1, \ldots, q_{3N}$, for which the motion in the first coordinate q_1 has quantum–mechanical character, while motion in the other coordinates is classical. For simplicity we consider only one quantum degree of freedom (DOF), but the derivation can be easily extended to a multidimensional quantum subsystem. It is assumed that the quantum DOF behaves as an oscillator with frequency much higher than $k_B T/h$, so that it is continuously in its ground state, and adjusts adiabatically to the change in classical coordinates. This is equivalent to treating the quantum DOF in the Born–Oppenheimer approximation, usually assumed to be valid for electronic degrees of freedom.

The quantum degree of freedom does not necessarily coincide with a generalized coordinate q_1, which would typically be the length of a covalent bond. The quantum degree of freedom would then represent the deviation from the position of minimum energy, which by itself is a function of the classical environment. In order to separate the quantum DOF it is therefore necessary to introduce an extra degree of freedom by splitting q_1 into a classical part q_1^0 and a quantum part ξ

$$q_1 = q_1^0 + \xi. \tag{1}$$

Simultaneously, we impose an extra condition, described below [Eq. (7)], which allows us to derive q_1^0 as a function of the state point in phase space of the classical system. Thus the total number of DOFs does not change.

We define the following column vectors:

$$\mathbf{q} = (q_1, q_2, \ldots, q_{3N})^T, \tag{2}$$

$$\mathbf{q}^0 = (q_1^0, q_2, \ldots, q_{3N})^T. \tag{3}$$

The Lagrangian of the system reads

$$L(\mathbf{q}, \dot{\mathbf{q}}) = \tfrac{1}{2}\dot{\mathbf{q}}^T \mathbf{M} \dot{\mathbf{q}} - V(\mathbf{q}) \tag{4}$$

$$= \tfrac{1}{2}M_{11}\dot{\xi}^2 + (\mathbf{M}\dot{\mathbf{q}}^0)_1 \dot{\xi} + \tfrac{1}{2}\dot{\mathbf{q}}^{0T}\mathbf{M}\dot{\mathbf{q}}^0 - V(\xi, \mathbf{q}^0), \tag{5}$$

where $\mathbf{M}$ is the symmetric $3N \times 3N$ mass-metric tensor, defined in terms of particle masses m_i and Cartesian coordinates x_i as

$$M_{kl} = \sum_i m_i \frac{\partial x_i}{\partial q_k} \frac{\partial x_i}{\partial q_l}. \tag{6}$$

In order to uncouple the quantum and classical motions, we now impose the condition that at all times

$$(\mathbf{M}\dot{\mathbf{q}}^0)_1 \equiv c, \tag{7}$$

where c is an arbitrary constant. Under this condition the conjugate momenta are defined by

$$p_\xi = \frac{\partial L}{\partial \dot{\xi}} = M_{11}\dot{\xi} + c, \tag{8}$$

$$\mathbf{p}^0 = \frac{\partial L}{\partial \dot{\mathbf{q}}^0} = \mathbf{M}\dot{\mathbf{q}}^0. \tag{9}$$

Note that condition (7) makes p_1^0 constant.

In the Hamiltonian representation, and imposing the condition with a Lagrange multiplier λ, we obtain the following modified Hamiltonian

$$H' = H + \lambda p_1^0 = \tfrac{1}{2}(M_{11})^{-1}p_\xi^2 - \tfrac{1}{2}(M_{11})^{-1}c^2$$
$$+ \tfrac{1}{2}\mathbf{p}^{0T}\mathbf{M}^{-1}\mathbf{p}^0 + V(\xi, \mathbf{q}^0) + \lambda p_1^0 \tag{10}$$

with the condition $p_1^0 \equiv c$. Therefore

$$\dot{q}_1^0 = \frac{\partial H}{\partial p_1^0} + \lambda. \tag{11}$$

Thus the Lagrange multiplier allows to set the velocity of q_1^0 to any value and thus manipulate q_1^0. A sufficient and necessary condition for the time derivative of p_1^0 to vanish is the following:

$$\dot{p}_1^0 = \frac{\partial H}{\partial q_1^0} = 0 \Leftrightarrow \frac{\partial H}{\partial q_1} = \frac{\partial H}{\partial \xi} = 0. \tag{12}$$

This means that q_1^0 is the value of q_1 for which the generalized force on q_1 vanishes; i.e., $-\partial H/\partial q_1 = 0$; thus,

$$-\mathbf{p}^{0T}\frac{\partial \mathbf{M}^{-1}}{\partial q_1}\mathbf{p}^0 - \frac{\partial V}{\partial q_1} = 0. \tag{13}$$

As seen in this equation, the generalized force is the sum of the velocity-dependent force (e.g., a centrifugal force) and the potential force. In practice an iterative procedure is needed in each integration step to set q_1^0 to the value of q_1 where the generalized force vanishes. For this value of q_1^0, the partial derivative to ξ of the Hamiltonian Eq. (10) also vanishes. Therefore the Hamiltonian in ξ contains only quadratic and higher-order terms in ξ and has the form

$$H(p_\xi,\xi)=\tfrac{1}{2}(M_{11})^{-1}p_\xi^2+H_0+\tfrac{1}{2}H''\xi^2+\dots, \qquad (14)$$

where H_0 is the value of the classical Hamiltonian $\tfrac{1}{2}\mathbf{p}^{0T}\mathbf{M}^{-1}\mathbf{p}^0+V(\mathbf{q})$ (disregarding the irrelevant constant term) at the value of q_1 where the generalized force vanishes, which is the energy of the classical system. Solving the time-independent Schrödinger equation for ξ we can construct the ground state solution, which has an energy equal to H_0 plus the zero-point energy of the quantum oscillator. The quantum solution depends parametrically on the classical coordinates and momenta $\mathbf{q}^0,\mathbf{p}^0$.

We now wish to treat the total system as a reduced dynamic system ($\mathbf{q}^0$) with flexible constraint, i.e., with the condition $p_1^0\equiv c$, omitting the quantum degrees of freedom. In order to preserve the correctness of thermodynamic quantities, the potential of the reduced system must be replaced by a potential of mean force V^{mf} with respect to the omitted degree of freedom

$$V^{\mathrm{mf}}(\mathbf{q}^0)=-k_BT\ln Q^{qm}=-k_BT\ln\sum_n e^{-E_n/k_BT}, \qquad (15)$$

where E_n are the solutions of $\hat{H}\psi_n=E_n\psi_n$. For a harmonic oscillator with frequency ν the potential of mean force becomes

$$V^{\mathrm{mf}}=h_0+\tfrac{1}{2}h\nu+k_BT\ln(1-e^{-h\nu/k_BT}). \qquad (16)$$

Since ν is a function of the state of the system in phase space, $\partial\nu/\partial\mathbf{q}^0$ leads to classical forces and to energy exchange between the quantum oscillator and the classical system. These forces are rather difficult to evaluate. However, in the case where $h\nu\gg k_BT$, only the zero-point energy survives. If the q dependence of ν can be neglected, the quantum degree of freedom adds a constant term that has no influence on the dynamics of the classical system.

So, for this case the effective Hamiltonian for the classical flexible-constraint dynamics is

$$H(\mathbf{p}^0,\mathbf{q}^0)=\tfrac{1}{2}\mathbf{p}^{0T}\mathbf{M}^{-1}\mathbf{p}^0+V(\mathbf{q}^0) \qquad (17)$$

under the condition

$$p_1^0\equiv c,$$

implying

$$\left(\frac{\partial H}{\partial q_1}\right)_{q_1^0}\equiv0. \qquad (18)$$

Note that this dynamic preserves the correctness of ensemble averages. There is no need for metric tensor corrections that have been discussed when hard degrees of freedom are replaced by constraints.[32]

The multidimensional case with n quantum DOFs $q_i=q_i^0+\xi_i$, $i=1,\dots,n$, leads to a straightforward extension. In that case there are n additional degrees of freedom and n conditions requiring that $\partial H/\partial q_i$ vanishes at $q_i=q_i^0$, $i=1,\dots,n$. The conditions $p_i^0\equiv c_i$ remove the coupling between quantum and classical degrees of freedom. The quantum subsystem now contains coupling terms between ξs and represents a system of coupled harmonic oscillators. In the case of ground state occupation with fixed frequencies, only a constant term is added to the classical Hamiltonian.

We now consider the practical case that the n quantum degrees of freedom concern distances between particles. This applies directly to bond constraints, but additional bond angle constraints can also be formulated in terms of a distance between two particles

$$q_i=||\mathbf{r}_{a(i)}-\mathbf{r}_{b(i)}||, \quad i=1,\dots,n. \qquad (19)$$

The now classical DOFs $q_k^0+\xi_k$, $k=1,\dots,n$ can be treated as flexible constraints. At each point in time the length of the constraints is such that condition (18) holds. This means that the total potential force and the centripetal force working in the direction of the constraint cancel out. Such a constraint keeps the derivative of the total energy H zero in the n constraint directions, while it should conserve angular momentum:

$$\begin{cases}\dfrac{\partial}{\partial q_i}H(\mathbf{r},\mathbf{v})=\dfrac{\partial}{\partial q_i}\left(\dfrac{1}{2}\mu_iq_i^2\omega_i^2+V(\mathbf{r})\right)=0\\[2mm]\dfrac{\partial}{\partial q_i}\mu_iq_i^2\omega_i=0\end{cases}$$
$$i=1,\dots,n, \qquad (20)$$

where $\mathbf{v}$ are the velocities and μ_i is the reduced mass of the two particles in constraint i

$$\mu_i=\frac{m_{a(i)}m_{b(i)}}{m_{a(i)}+m_{b(i)}} \qquad (21)$$

and ω_i is the angular velocity of constraint i

$$\omega_i=\frac{||\mathbf{v}_{a(i)}-\mathbf{v}_{b(i)}||}{q_i}. \qquad (22)$$

In Eq. (20) we have substituted the total kinetic energy by the rotational energy of constraint i, using condition (18). The gradient of the potential can be evaluated using Eq. (19)

$$\begin{cases}\dfrac{\partial}{\partial q_i}H(\mathbf{r},\mathbf{v})=\mu_iq_i\omega_i^2+\mu_iq_i^2\omega_i\dfrac{\partial\omega_i}{\partial q_i}-\mathbf{f}(\mathbf{r})\cdot\dfrac{\partial\mathbf{r}}{\partial q_i}=0\\[2mm]\dfrac{\partial}{\partial q_i}\mu_iq_i^2\omega_i=0\end{cases}$$
$$i=1,\dots,n, \qquad (23)$$

where $\mathbf{f}(\mathbf{r})=-\nabla V(\mathbf{r})$ is the force. The derivative $\partial\omega_i/\partial q_i$ can be obtained from the condition of conserved angular momentum and substituted to arrive at the constraint

$$-\mu_iq_i\omega_i^2-\mathbf{f}(\mathbf{r})\cdot\frac{\partial\mathbf{r}}{\partial q_i}=0 \quad i=1,\dots,n. \qquad (24)$$

This means the total potential force and the centrifugal force working in the direction of the constraint cancel out. When

the potential in the direction of the constraint is narrow, such as a bond potential, the major difference with a rigid constraint is that the latter does not take up energy, while for a flexible constraint energy is divided equally between rotational kinetic energy and potential energy in the constraint direction.

Zhou et al.[31] introduced two different methods that solve the equations of motion with flexible constraints. However, both methods only solve the equations in an approximate way, because only a harmonic bond potential is considered in the adjustment of the bond lengths at each integration step. This assumes the other contributions to the second derivative of the potential in the bond directions are negligible. It is also limited to harmonic bond potentials. Method I of Zhou et al. uses a second set of Lagrange multipliers at each integration step. The result is a non-Hamiltonian set of equations. Method II ignores the kinetic contributions. This leads to a Hamiltonian system with a symplectic integration scheme. Both methods are time reversible and conserve linear and angular momentum.

We propose a method that is similar to method I of Zhou et al., but which works for any combination of coupled constraints and with the full potential that works in the direction of the bond. It does not require complicated mathematics for evaluating the rotational forces, since these are calculated from constraint displacements.

III. THE ALGORITHM

The algorithm is written for a leap-frog integrator, but it also works for a velocity Verlet integrator. First we do a normal constrained update step:

$$\mathbf{r}_{n+1}^{0'}=\mathbf{r}_n+h(\mathbf{v}_{n-(1/2)}+h\mathbf{M}^{-1}\mathbf{f}_n),\tag{25}$$

$$\text{CONSTRAIN}(\mathbf{r}_n,\mathbf{r}_{n+1}^{0'},\mathbf{r}_{n+1}^0),\tag{26}$$

$$\mathbf{v}_{n+(1/2)}^0=\frac{1}{h}(\mathbf{r}_{n+1}^0-\mathbf{r}_n),\tag{27}$$

where h is the time step, $\mathbf{M}$ is a $3N\times3N$ diagonal matrix containing the masses of the particles, a subscript denotes the MD step number, and a prime unconstrained coordinates. CONSTRAIN($\mathbf{r},\mathbf{s},\mathbf{t}$) means that coordinates $\mathbf{s}$ are constrained using the directions and the lengths of the constraints in $\mathbf{r}$ and the result is written to $\mathbf{t}$. For this we used the LINCS algorithm.[35] These coordinates and velocities are used to start an iterative minimization. In iteration i of the minimization we need to calculate the kinetic and the potential forces working in the direction of the constraints. The rotational acceleration in the direction of the constraints $\boldsymbol{\phi}_{n+1}^i$ is calculated by doing one step backward and another one forward in time:

$$\mathbf{x}_{-1}^{i'}=\mathbf{r}_{n+1}^i-\frac{1}{h}\mathbf{v}_{n+(1/2)}^0,\tag{28}$$

$$\text{CONSTRAIN}(\mathbf{r}_{n+1}^i,\mathbf{x}_{-1}^{i'},\mathbf{x}_{-1}^i),\tag{29}$$

$$\mathbf{x}_{+1}^{i'}=\mathbf{r}_{n+1}^i+h\left(\mathbf{v}_{n+(1/2)}^0+h\mathbf{M}^{-1}\mathbf{f}_{n+1}^i\right),\tag{30}$$

$$\text{CONSTRAIN}(\mathbf{r}_{n+1}^i,\mathbf{x}_{+1}^{i'},\mathbf{x}_{+1}^i),\tag{31}$$

$$\boldsymbol{\phi}_{n+1}^i=\frac{1}{h^2}(2\mathbf{r}_{n+1}^i-\mathbf{x}_{-1}^i-\mathbf{x}_{+1}^i).\tag{32}$$

Note that $\boldsymbol{\phi}_{n+1}^i$ will also contain a component that is perpendicular to the constraints, but this component will be removed in the next step. The important point is that $\boldsymbol{\phi}_{n+1}^i$ only contains the rotational acceleration and no other terms that work in the direction of the constraints. To conserve angular momentum we should move the particles in the direction of the old constraints, just like in a normal leap-frog constraint step:

$$\text{PROJECT}(\mathbf{r}_n,\boldsymbol{\phi}_{n+1}^i+\mathbf{M}^{-1}\mathbf{f}_{n+1}^i,\mathbf{a}_{n+1}^i),\tag{33}$$

where PROJECT($\mathbf{r},\mathbf{s},\mathbf{t}$) means that $\mathbf{s}$ is projected on the constraints in $\mathbf{r}$ and the result is written to $\mathbf{t}$. For this we also used the LINCS algorithm. We now have the total acceleration $\mathbf{a}_{n+1}^i$ that works in the direction of the old constraints. The magnitude of the acceleration almost does not change when using the old instead of the new constraint direction, since the constraints rotate over a very small angle in one MD step. The minimization has converged when the average force in the direction of the constraints is smaller than a predefined tolerance:

$$\frac{1}{M}||\mathbf{M}\,\mathbf{a}_{n+1}^i||<f_{\text{tol}}.\tag{34}$$

When it has not converged we do a step in the direction of the acceleration

$$\mathbf{r}_{n+1}^{i+1}=\mathbf{r}_{n+1}^i+\frac{1}{k}\mathbf{a}_{n+1}^i,\tag{35}$$

where k is a constant with unit one over time squared. For rapid convergence, this constant should be chosen as

$$k=\frac{1}{\mu_i}\frac{\partial^2 V}{\partial q_i^2}.\tag{36}$$

If the value of k is not equal for all q_i's, a reasonable value can be obtained by trying several intermediate values. When the minimization has converged, the new coordinates, the velocities at the half step, and the new forces are given by

$$\mathbf{r}_{n+1}=\mathbf{r}_{n+1}^i,\tag{37}$$

$$\mathbf{v}_{n+(1/2)}=\frac{1}{h}(\mathbf{r}_{n+1}-\mathbf{r}_n),\tag{38}$$

$$\mathbf{f}_{n+1}=\mathbf{f}_{n+1}^i.\tag{39}$$

Just like method I of Zhou et al.,[31] this method is time reversible and conserves linear and angular momentum. The method is computationally much more expensive than normal MD, because all the forces need to be evaluated once during each iteration of the minimization, the computational cost of the rest of the algorithm being negligible. But when used in combination with a model requiring a minimization procedure for polarization, it can be done almost for free,
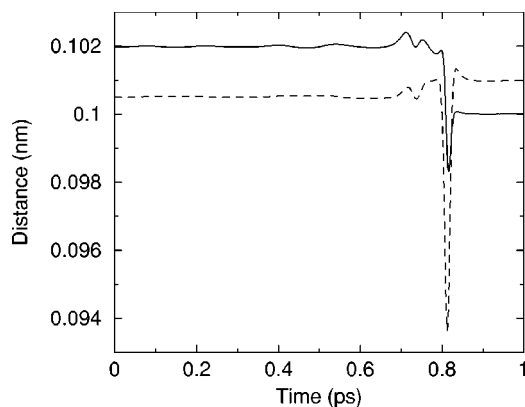
FIG. 1. The distance between the particles in first dumbbell (solid line) and between the particles in the second (dashed line) dumbbell.

FIG. 2. The total (dashed line) and kinetic energies (solid line) of the dumbbell system.

since both minimizations can be done at the same time. For a polarizable model using shells, the forces on the shells can be added to the forces in the constrained directions in the convergence criterion Eq. (34). The shells are displaced by adding the forces on the shells divided by the shell spring constant to the right of Eq. (35).

IV. TEST CASE

A. Collision of two rotating dumbbells

As a simple two-dimensional test system we used two rotating dumbbells, which is analogous to system (A) of Zhou et al.[31] Each dumbbell consists of two Lennard-Jones (LJ) particles connected by a spring with a force constant of $10\,000$ kJ mol^{-1} nm^{-1}. The bond lengths and the sigmas of the LJ potential are 0.1 nm. The depth of the LJ potential is 0.25 kJ mol^{-1}. The two dumbbells are initially separated by a small distance and one is rotating twice as fast as the other. Because of the Lennard-Jones attraction they collide after a few rotations and the direction of rotation of the fastest rotating dumbbell is inverted. The distances between the particles in each dumbbell are shown in Fig. 1.

Initially the springs are stretched due to the centrifugal force. Because the first dumbbell rotates twice as fast as the second, the kinetic force is four times as large and the spring stretches four times as much. The collision and change of direction of rotation occur just after 0.8 ps. There the springs contract due to the repulsive interaction at short distance with a particle of the other dumbbell. The total and kinetic energies of the system are shown in Fig. 2. The collision and change of direction of rotation occur just after 0.8 ps. The energy conservation at the collision can be seen in more detail in Fig. 3. The fluctuations in the energy are of the order of the accuracy of the kinetic energy in the leap-frog algorithm. The actual accuracy of the integrator can be determined from the difference in the total energy at time 0 and 1 ps, where the kinetic and potential energies are almost constant. This difference is 3×10^{-5} kJ mol^{-1}. Also shown in Fig. 3 is the total energy for the algorithm where ϕ_{n+1}^0 is used during the minimization instead of ϕ_{n+1}^{i+1}. This leads to a jump in the energy, thus losing time reversibility.
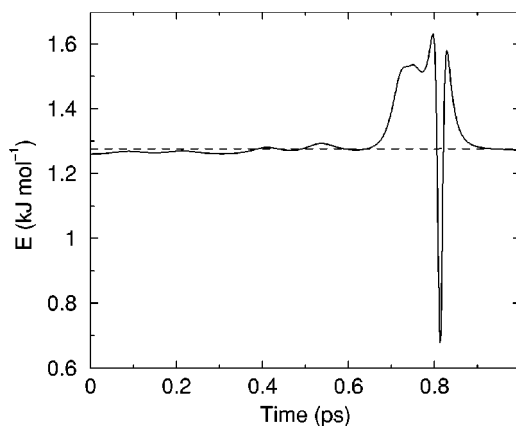
V. APPLICATIONS

A. Liquid water with the MCDHO model

In this section we show a more interesting application of flexible constraints. In the liquid, the intramolecular DOFs of the water molecules are in their respective ground states; but the molecules are deformed with respect to the gas-phase geometry,[36–38] where the protons should adiabatically reach the positions that minimize the potential energy of the intramolecular DOFs, subject to the interactions with the other molecules and to centrifugal forces.

When intramolecular DOFs are included explicitly, it is also convenient to explicitly account for the electronic polarizability, because the effects are of similar magnitude.[18] These features should not be superimposed on an empirically fitted model, that has ''parametrized them away'' and thus would be overcorrected. Instead, a model is required that can reliably reproduce the water molecule in the gas phase, and includes polarizability and flexibility. One such model is MCDHO,[34] whose intramolecular parameters were fitted to a high-quality surface of the energetic cost of deformation.[39]

The MCDHO model consists of three cores or particles and a shell, which models the electron cloud of the oxygen as a spherical, exponentially decaying charge density (see Fig. 4). Each core has a positive charge and interacts elec-
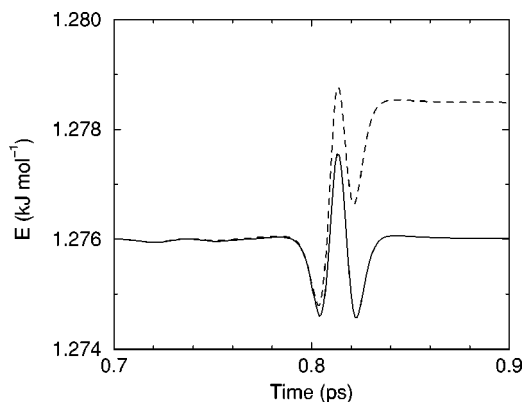

FIG. 3. The total energy of the dumbbell system with the rotational force determined at each step of the minimization (solid line) or only determined at the first step of the minimization (dashed line).
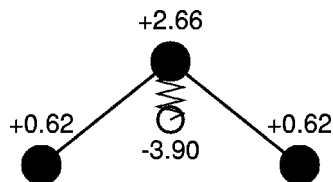
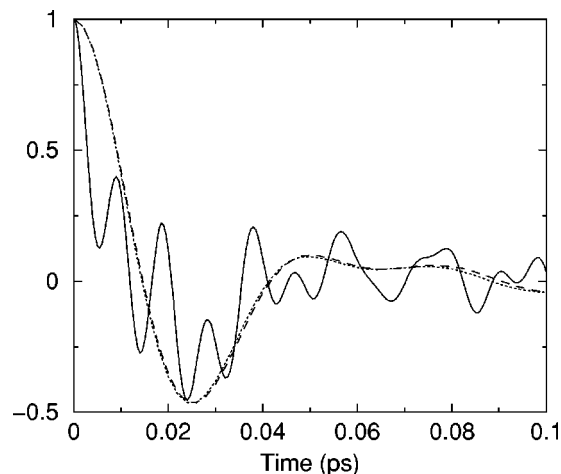FIG. 4. The MCDHO water model with the charges on the four sites.

FIG. 5. The velocity autocorrelation function of the hydrogens in the MCDHO model for the MD–FF (solid line), the MD–RC (dotted line), and the MD–FC (dashed line) simulations.

trostatically with all the other cores in the system. Core–core Lennard-Jones terms are used for intermolecular interactions only, whereas within the same molecule the oxygen is connected to the hydrogens with Morse potentials, and a fourth order expression is used for the bending potential of the H–O–H angle. The shell is massless and it adiabatically reaches the position that minimizes its contribution to the potential energy of the system. The shell has a negative charge and interacts electrostatically with all the cores in the system, apart from the oxygen in the same molecule, to which it is attached by a harmonic spring. Because the shell is a charge density, the shell–core electrostatic interactions are screened. However, the shell–shell interactions are not screened, but instead have Lennard-Jones terms. The intermolecular parameters of the model were fitted to reproduce the interaction energy and the geometry of the optimum water dimer.[40,41]

Thus, the potential in the direction of an O–H bond consists of a Morse potential, intramolecular electrostatic interactions, and intermolecular interactions. Although the first two mainly determine the distribution of O–H distances, the external contribution cannot be neglected, as shown by the experimentally observed lengthening of the O–H bonds in the liquid.[36–38] The H–O–H angle is also a fast degree of freedom with quantum nature, whose value is modified by the intermolecular interactions. Hence, in the following MD simulations both the O–H and the H–H distances are treated similarly: as classical DOFs, in a first one; as rigid constraints, in a second one, and as flexible constraints in a third one. The ground state assumption is quite satisfied with $h\nu/k_B T = 17$ for bond vibrations and $h\nu/k_B T = 8$ for angle-bending vibrations.

B. Simulations

We performed three simulations of 1000 MCDHO molecules in a periodic cubic box at a fixed density of 997 kg m^{-3}. A Berendsen thermostat[42] with a coupling time of 0.1 ps was used to maintain the temperature at $T = 298$ K. The cutoff for the particle–particle interactions was 1 nm, the long-range electrostatics were treated with the particle mesh Ewald method (PME)[43] and a dispersion correction was applied for the Lennard-Jones interactions. The neighbor list was updated at each integration step. The force tolerance for the minimization of the shells was 0.1 kJ mol^{-1} nm^{-1} for all three simulations.

The first simulation produced classical trajectories for all the DOFs of the nuclei, including bond, and bond angle vibrations, so it required a short time step of 0.5 fs. This we call the fully flexible (FF) simulation and denote it as MD–FF. The average value of the O–H distance resulted 0.0985

nm and of the H–H distance, 0.1538 nm, with standard deviations of 0.0026 and 0.0053 nm, respectively. However, the centers of Gaussian fits to their distributions were 0.1 pm shorter, 0.0984 nm for O–H and 0.1537 for H–H.

In the second simulation, the intramolecular DOFs were constrained to the two latter values and a time step of 2 fs was used. This is the rigidly constrained (RC) simulation MD–RC. Finally, flexible constraints (FCs) were used in the third simulation, hereafter denominated MD–FC, also with a time step of 2 fs. The force tolerance for the minimization of the FCs was the same as that for the shells, 0.1 kJ mol^{-1} nm^{-1}. Both simulations with constraints were equilibrated for 10 ps after starting from an equilibrated conformation from the first one.

C. Fast dynamics

To look at fast dynamics we performed three short simulations of 2 ps each. The fastest motions can be found by looking at the velocity autocorrelation function of the Cartesian velocities of the hydrogens (see Fig. 5). In MD–FF, the first peak appears at 9 fs, which corresponds to one period of the bond vibrations. The velocity autocorrelation functions for MD–RC and MD–FC are almost identical, with the first peak at 50 fs, which corresponds to the libration of the molecule. The integration is accurate for all three simulations, MD–FF having 18 integration steps per period of the fastest oscillation, whereas for MD–RC and MD–FC this number is 25. The average number of force evaluations per step is 14 for MD–FF simulation, 16 for MD–RC and 19 for MD–FC. The constrained simulations are computationally much more efficient than the flexible one, because the time step can be chosen four or five times as large.

D. Thermodynamics and structure

To obtain thermodynamic properties and the slow dynamics we extended the three simulations to 80 ps. One check for the integration accuracy is the temperature of the system. The Berendsen thermostat tries to keep the tempera-

ture constant at 298 K, but if heat is continuously flowing in or out of the system, this will cause a temperature difference proportional to the heat flow. The temperature is 298.0, 297.8, and 297.4 K for MD–FF, MD–RC and MD–FC, respectively. All deviations are relatively small. We also checked for equipartition, which was completely fulfilled in the three simulations.

The potential energy per molecule in the liquid (subtracting the energy of a monomer) of MD–FF resulted in -43.3 kJ mol^{-1}, slightly different from that previously reported,[34] -43.5 kJ mol^{-1}. This latter value was obtained from a MC simulation, without using a dispersion correction, that should have lowered the energy to -43.8 kJ mol^{-1}. The small difference of 0.5 kJ mol^{-1} with the MD–FF energy is probably due to an error in the treatment of the screening in the PME algorithm in the MC code.

The value that resulted from MD–RC was -46.8 kJ mol^{-1}, and from MD–FC was -46.9 kJ mol^{-1}. The difference relative to the flexible simulation corresponds to the loss of the thermal motion in the three constrained degrees of freedom, which contributes $3 k_B T/2 = 3.7$ kJ mol^{-1} to the potential energy. Our results can be compared to the value -47.4 kJ mol^{-1} from a recent simulation with 125 MCDHO water molecules.[30] The small difference is due to the smaller number of molecules; in the same work, the result for 512 molecules is -47.0 kJ mol^{-1}. Using the quantum corrections reported from the PIMD simulation,[30] together with the common assumptions[44] that the gas behaves ideally and that the liquid is incompressible, the vaporization enthalpy predicted from our simulations is $\Delta H_{vap} = 43.2$ kJ mol^{-1}, which falls somewhat short from the experimental value[45] $\Delta H_{vap} = 44.0$ kJ mol^{-1}.

The O–H and H–H distance distributions in both MD–FF and MD–FC are almost perfect Gaussians (see Fig. 6). In the latter case the average and standard deviation of the distributions are identical to those of the Gaussian fits: $\langle r_{OH} \rangle = 0.0982$ nm, $\Delta r_{OH}^{rms} = 0.0009$ nm, and $\langle r_{HH} \rangle = 0.1534$ nm, $\Delta r_{HH}^{rms} = 0.0019$ nm. Both distances are slightly shorter (~ 0.3 pm) than in the former case, and the widths of their distributions are three times smaller. The average H–O–H angle predicted from this values is 102.7°, which matches quite well the experimental data of Thiessen and Narten,[36] but is smaller than the more recent experimental data of Ichikawa et al.[37] (see Table I). This discrepancy is common to other flexible potentials.[18,19,29] Because the same widening of the H–O–H angle of the water molecule in the liquid has been predicted with quantum calculations,[46,47] and the MCDHO model consistently produced H–O–H angles smaller than, as well as O–H bond lengths longer than the *ab initio* results for all the clusters with which it was compared,[34] it seems to exaggerate the intermolecular O–H attraction and the H–H repulsion.

The $g_{OO}(r)$ radial distribution functions for the three simulations are shown in Fig. 7. It can be seen that they are almost identical, with a 2% variation in the height of the first maximum and the depth of the first minimum, overestimated for MD–RC, and underestimated for MD–FC. The difference resulted in being even smaller for $g_{OH}(r)$ and $g_{HH}(r)$ (data not shown). Therefore, the changes in the structure of
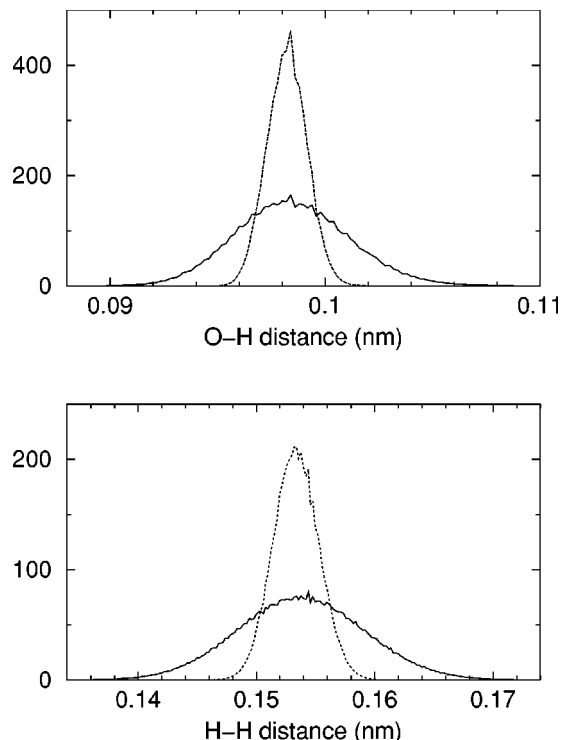

FIG. 6. The O–H distance (top graph) and H–H distance (bottom graph) distributions of the MCDHO water model for the MD–FF (solid lines) and the MD–FC (dotted lines) simulations.

the liquid observed in the PIMD simulation[30] are due exclusively to quantum effects.

E. Slow dynamics

In contrast to the static behavior and the fast dynamics, the slow dynamic properties do change significantly, as can be seen from the rotational correlation times and the diffusion coefficients in Table II. The latter were determined from the mean square displacement by fitting a straight line from time 5 to 50 ps. The error was determined by the difference of the fits over the two halves of the interval.

All dynamical quantities reported in Table II scale consistently between the simulations. MD–RC yielded the slowest dynamics, followed by MD–FF; the use of flexible con-

TABLE I. Geometry of the water molecule in the liquid.

Method	$\langle r_{OH} \rangle$ (nm)	$\langle r_{HH} \rangle$ (nm)	$\angle HOH^a$ (deg)
MD–FF[b]	0.0985	0.1538	102.7°
MD–FC[b]	0.0982	0.1534	102.7°
Experimental[c]	0.0966(6)	0.151(3)	102.8°
Experimental[d]	0.0970(5)	0.155(1)	106.1°
QM[e]	0.0941	⋯	106.2°
QM[f]	0.0988	⋯	106.7°

[a]The angles were computed from the reported distances.
[b]This work.
[c]Neutron diffraction experiment with mixtures of light and heavy water (see Ref. 36).
[d]Neutron diffraction experiment with heavy water (see Ref. 37).
[e]Simulation of a quantum molecule in a classical liquid (see Ref. 46).
[f]Calculation of a quantum molecule in an average reaction field (see Ref. 47). The number in parentheses denotes the uncertainty in the last digit.
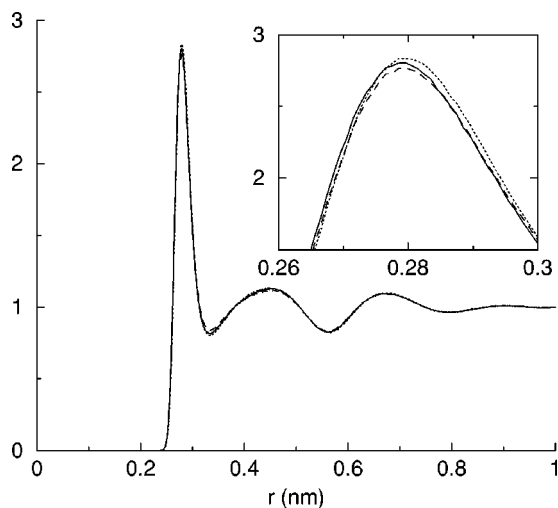
FIG. 7. The radial distribution function of the oxygens in MCDHO water for the MD–FF (solid line), the MD–RC (dotted line), and the MD–FC (dashed line) simulations.

straints produced a speedup of 25% with respect to the former, and of 11% with respect to the latter. Nevertheless, the classical prediction of the MCDHO model dynamics is still slower than real water by a factor of 2. However, PIMD simulations with flexible versions of the simple point charge (SPC) model have shown an increase of up to 73% in the diffusion constant, due to quantum effects.[29] If quantum effects on diffusion, which are mainly due to shifts in zero point energy in translational and librational modes, were that strong the value for the MCDHO model would become $D = 2 \times 10^{-9}$ $m^2 s^{-1}$, which is much closer to experimental values. The experimental diffusion constant for D_2O is indeed lower than for H_2O, but the difference is less than 10%, indicating a much smaller quantum effect. A study of these quantum effects for the MCDHO model has not been done and is beyond the aim of the present work.

VI. DISCUSSION

We showed that flexible constraints are the thermodynamically correct replacements for hard quantum degrees of freedom, and presented an algorithm for flexible constraints that works for any combination of coupled distance con-

straints. The algorithm is time reversible and conserves energy and linear and angular momenta, as shown by a simple test case.

The application of the method to the study of liquid water under ambient conditions showed that the thermodynamic properties and the structure of the liquid were not sensitive to whether the simulation included the intramolecular degrees of freedom, or if they were treated as rigid or flexible constraints.

The dynamics, however, differs considerably: Flexible constraints resulted in a 10% speedup with regard to the flexible simulation, and a 25% speedup with respect to the rigidly constrained one. As a flexible constraint is a better approximation of a chemical bond, the other two representations significantly underestimate the rate of the dynamic quantities in small molecules.

For nonpolarizable models the algorithm is computationally expensive, because all forces on the constraints need to be evaluated in each iteration of the minimization; but when used in combination with a polarizable model having shells whose positions need to be optimized in each step, there is almost no extra computational cost. In this case both flexible and rigid bond constraints can speed up simulations significantly, as larger time steps can be used. As the number of iterations for the rigidly constrained and flexibly constrained simulations is comparable, flexible constraints can be used without extra cost.

The replacement of hard quantum degrees of freedom by flexible constraints neglects the configuration dependence of the zero-point energy, which in the case of water is not vanishingly small. It is possible to correct for zero-point energies, at least within the harmonic approximation and to first order, if the three fundamental vibrational frequencies of the water molecule are computed at each step, based on the knowledge of the Hessian for the internal degrees of freedom. This has the additional advantage that the spectral shapes for the intramolecular vibrational bands of the liquid are obtained as well, but it adds considerably to the complexity of the simulation.

With regard to the MCDHO model, we found its dynamics to be slow compared to that of real water. Quantum effects, though, are expected to yield faster dynamics.[29] Opposite to experimental data and quantum calculations, the H–O–H angle of the MCDHO model in the liquid is smaller than in the gas. We hint that this might be corrected by a refinement in the intermolecular O–H and H–H interactions. This might also correct the deviations relative to the experimental data of the radial distribution function that have been reported.[30,34] However, such a refinement is well beyond the aims of the present work.

VII. CONCLUSIONS

As the computational capacities and the understanding of molecular interactions increase, so does the possibility of using more complex models in numerical simulations of large molecular systems. Care must be taken, though, that the inclusion of fast degrees of freedom is done properly. This requires new methods that are theoretically sound and, preferably, simple and easy to implement.

TABLE II. Dynamical properties for the three different MD simulations with the MCDHO model. From left to right, the rotational correlation times using $\cos \theta$ for averaging, for the H–H vector (τ_1^{HH}), the dipole moment (τ_1^μ), and the normal to the water plane ($\tau_1^\perp$). τ_2^{HH} is the correlation time using $3 \cos^2 \theta - 1$ for averaging and D is the diffusion constant. The rotational correlation times were obtained by integrating the rotation autocorrelation function with an exponential fit for the tail. The experimental values for τ_2^{HH} and D are from Refs. 48 and 49, respectively. The number in parentheses denotes the uncertainty in the last digit.

Method	τ_1^{HH} (ps)	τ_1^μ (ps)	$\tau_1^\perp$ (ps)	τ_2^{HH} (ps)	D ($\times 10^{-9}$ $m^2 s^{-1}$)
MD–FF	8.7	8.6	5.8	4.3	1.09(2)
MD–RC	10.1	11.0	7.0	4.8	0.92(3)
MD–FC	8.0	8.4	5.7	3.6	1.16(2)
Experimental				2.0	2.4

In this work we have addressed the problem of decoupling the intramolecular vibrations, which should be treated quantum mechanically, from other molecular motions that are adequately described with classical mechanics, but without losing the advantages of a flexible model that includes the effects of molecular deformations. We showed that the assumption of high frequencies for the quantum DOFs allows the derivation of Hamiltonian equations of motion for the classical DOFs, as long as the quantum DOFs adiabatically reach their equilibrium values, which are determined by the intramolecular and intermolecular interactions. Then we presented an algorithm that can easily be implemented in a MD program, and has very good conservation properties, as shown from its application to a simple test case. Finally, we used the method in a study of liquid water under ambient conditions, with a flexible and polarizable model, from which we show the effects of flexible constraints in the dynamical properties. The analysis of the structural data provides basis to hint at possible refinements of the MCDHO model.

ACKNOWLEDGMENTS

[1] M. P. Allen and D. J. Tildesley, *Computer Simulations of Liquids* (Oxford Science, Oxford, 1987).
[2] D. Frenkel and B. Smit, *Understanding Molecular Simulations: From Algorithms to Applications* (Academic, New York, 1996).
[3] I. G. Tironi, R. M. Brunne, and W. F. van Gunsteren, Chem. Phys. Lett. **250**, 19 (1996).
[4] J. P. Ryckaert, G. Ciccotti, and H. J. C. Berendsen, J. Comput. Phys. **23**, 327 (1977).
[5] H. C. Andersen, J. Comput. Phys. **52**, 24 (1983).
[6] S. Miyamoti and P. A. Kollman, J. Comput. Chem. **13**, 952 (1992).
[7] H. A. Stern, F. Rittner, B. J. Berne, and R. A. Friesner, J. Chem. Phys. **115**, 2237 (2001).
[8] W. F. van Gunsteren, Mol. Phys. **40**, 1015 (1980).
[9] D. M. Ferguson, J. Comput. Chem. **16**, 501 (1995).
[10] K. Ichikawa and Y. Kameda, J. Phys.: Condens. Matter **1**, 257 (1989).
[11] J. M. Martínez, J. Hernández-Cobos, H. Saint-Martin, R. R. Pappalardo, I. Ortega-Blake, and E. Sánchez-Marcos, J. Chem. Phys. **112**, 2339 (2000).
[12] D. A. Doyle, J. M. Cabral, R. A. Pfuetzner, A. Kuo, J. M. Gulbis, S. L. Cohen, B. T. Chait, and R. MacKinnon, Science **280**, 69 (1998).
[13] D. Meuser, H. Splitt, R. Wagner, and H. Schrempf, FEBS Lett. **462**, 447 (1999).
[14] K. Toukan and A. Rahman, Phys. Rev. B **31**, 2643 (1985).
[15] J. Anderson, J. J. Ullo, and S. Yip, J. Chem. Phys. **87**, 1726 (1987).
[16] L. X. Dang and B. M. Pettit, J. Phys. Chem. **91**, 3349 (1987).
[17] O. Teleman, B. Jönsson, and S. Engstrom, Mol. Phys. **60**, 193 (1987).
[18] G. Corongiu, Int. J. Quantum Chem. **42**, 1209 (1992).
[19] P. J. van Maaren and D. van der Spoel, J. Phys. Chem. B **105**, 2618 (2001).
[20] R. P. Feynman and A. R. Hibbs, *Quantum Mechanics and Path Integrals* (McGraw–Hill, New York, 1965).
[21] M. Parrinello and A. Rahman, J. Chem. Phys. **80**, 860 (1984).
[22] J. Cao and G. A. Voth, J. Chem. Phys. **99**, 10070 (1993).
[23] J. Cao and G. A. Voth, J. Chem. Phys. **100**, 5106 (1994).
[24] J. Cao and G. A. Voth, J. Chem. Phys. **101**, 6157 (1994).
[25] J. Cao and G. A. Voth, J. Chem. Phys. **101**, 6168 (1994).
[26] R. A. Kuharski and P. J. Rossky, Chem. Phys. Lett. **103**, 357 (1984).
[27] R. A. Kuharski and P. J. Rossky, J. Chem. Phys. **82**, 5164 (1985).
[28] G. S. D. Buono, P. J. Rossky, and J. Schnitker, J. Chem. Phys. **95**, 3728 (1991).
[29] J. Lobaugh and G. A. Voth, J. Chem. Phys. **106**, 2400 (1997).
[30] H. A. Stern and B. J. Berne, J. Chem. Phys. **115**, 7622 (2001).
[31] J. Zhou, S. Reich, and B. R. Brooks, J. Chem. Phys. **112**, 7919 (2000).
[32] S. Reich, Physica D **89**, 28 (1995).
[33] E. Lindahl, B. Hess, and D. van der Spoel, J. Mol. Model. [Electronic Publication] **7**, 306 (2001).
[34] H. Saint-Martin, J. Hernández-Cobos, M. I. Bernal-Uruchurtu, I. Ortega-Blake, and H. J. C. Berendsen, J. Chem. Phys. **113**, 10899 (2000).
[35] B. Hess, H. Bekker, H. J. C. Berendsen, and J. G. E. M. Fraaije, J. Comput. Chem. **18**, 1463 (1997).
[36] W. E. Thiessen and A. H. Narten, J. Chem. Phys. **77**, 2656 (1982).
[37] K. Ichikawa, Y. Kameda, T. Yamaguchi, H. Wakita, and M. Misawa, Mol. Phys. **73**, 79 (1991).
[38] A. K. Soper, Chem. Phys. **258**, 121 (2000).
[39] H. Partridge and D. W. Schwenke, J. Chem. Phys. **106**, 4618 (1997).
[40] M. Schütz, S. Brdarski, P. O. Widmark, R. Lindh, and G. Karlström, J. Chem. Phys. **107**, 4597 (1997).
[41] W. Klopper, J. G. C. M. van Duijneveldt-van de Rijdt, and F. B. van Duijneveldt, Phys. Chem. Chem. Phys. **2**, 2227 (2000).
[42] H. J. C. Berendsen, J. P. M. Postma, W. F. van Gunsteren, A. DiNola, and J. R. Haak, J. Chem. Phys. **81**, 3684 (1984).
[43] T. Darden, D. York, and L. Pedersen, J. Chem. Phys. **98**, 10089 (1993).
[44] W. L. Jorgensen, J. Chandrasekhar, J. D. Madura, R. W. Impey, and M. L. Klein, J. Chem. Phys. **79**, 926 (1983).
[45] G. S. Kell, J. Chem. Eng. Data **20**, 97 (1975).
[46] N. W. Moriarty and G. Karlström, J. Chem. Phys. **106**, 6470 (1997).
[47] T. M. Nymand and P. O. Åstrand, J. Phys. Chem. A **101**, 10039 (1997).
[48] B. Halle and H. Wennerström, J. Chem. Phys. **75**, 1928 (1981).
[49] K. Krynicki, C. D. Green, and D. W. Sawyer, Discuss. Faraday Soc. **66**, 199 (1978).